Inorg. Chem. **2005**, *44*, 7547−7558

Photon-, Electron-, and Proton-Induced Isomerization Behavior of Ferrocenylazobenzenes

Aiko Sakamoto,[†] Akira Hirooka,[†] Kosuke Namiki,[†] Masato Kurihara,[‡] Masaki Murata,[†] Manabu Sugimoto,[§] and Hiroshi Nishihara*[,†]

Department of Chemistry, School of Science, The University of Tokyo, Hongo, Bunkyo-ku, Tokyo 113-0033, Japan, Department of Biological Chemistry, Faculty of Science, Yamagata University, 1-4-12 Kojirakawa-machi, Yamagata 990-8560, Japan, and Department of Applied Chemistry and Biochemistry, Faculty of Engineering, Kumamoto University, Kurokami, Kumamoto 860-8555, Japan

Received July 15, 2005

3-, 4-, and 2-ferrocenylazobenzenes, **1**, **2**, and **3**, respectively, and several derivatives of **1** were synthesized, and their photoisomerization behaviors were examined. The molecular structures of **1** and its derivatives, 2-chloro-5-ferrocenylazobenzene (**5**) and 3-ferrocenyl-4′-hydroxylazobenzene (**11**), were determined by X-ray diffraction analysis. 3-Ferrocenyl compound **1** undergoes reversible trans-to-cis isomerization with a single green light source and the Fe^{III}/Fe^{II} redox change. 4- and 2-Ferrocenyl compounds, **2** and **3**, also respond to green light in addition to UV light, exciting the π–π^* transition, but the cis molar ratio in the photostationary state (PSS) is lower than that of **1**. The response to green light in **2** and **3** is caused by the MLCT (from Fe d orbital to azo π^* orbital) band excitation, while the character of the MLCT band, as estimated by time-dependent density functional theory calculations, differs between **1** and **2**. The oxidized form of **2** undergoes facile cis-to-trans thermal isomerization. Both **1** and **2** undergo facile protonation and show proton-catalyzed cis-to-trans isomerization. Among the derivatives of **1**, 2-chloro-5-ferrocenylazobenzene (**5**) exhibits the highest cis molar ratio (47%) in the PSS of green light irradiation.

Introduction

Among photochromic molecules whose structures and colors change reversibly by photoirradiation with alternating two kinds of light, azobenzene is one of the most popular. This compound has attracted much attention recently because of its possibilities of versatile applications to molecular memories and switches.[1] Combining azobenzene with metal complexes is noteworthy in view of the ability to exhibit novel functions deriving from the combination of redox, optical, and magnetic properties of the metal complexes with the photoisomerization of the azobenzene moiety. A number of photoisomerization studies of azo-conjugated metal complexes have been reported in recent years.[2] We have been systematically investigating the unique properties of azo-conjugated transition metal complexes.[3] One unique property is the reversible trans-to-cis isomerization of the azobenzene moieties using a combination of a single light source and the redox change of the metal complex moieties. We previously reported three different systems showing this phenomenon: tris(azobenzene-bound bipyridine)cobalt,[3h,3i] bis(azobenzene-bound bipyridine)copper,[3j] and 3-ferrocenylazo-

* Author to whom correspondence should be addressed. Phone: +81-3-5841-4346. Fax: +81-3-5841-8063. E-mail: nisihara@chem.s.u-tokyo.ac.jp.

[†] University of Tokyo.

[‡] Yamagata University.

[§] Kumamoto University.

(1) (a) Ikeda, T.; Tsutsumi, O. *Science* **1995**, *268*, 1873−1875. (b) Liu, Z. F.; Fujishima, A.; Hashimoto, K. *Nature* **1990**, *347*, 658−660. (c) Blanchard, P. M.; Mitchell, G. R. *Appl. Phys. Lett.* **1993**, *63*, 2038−2040.

(2) (a) Barlow, S.; Marder, S. R. *Chem. Commun.* **2000**, 1555−1562. (b) Yam, V. W. W.; Lau, V. C. Y.; Wu, L. X. *J. Chem. Soc., Dalton. Trans.* **1998**, 1461−1468. (c) Hayami, S.; Inoue, K.; Osaki, S.; Maeda, Y. *Chem. Lett.* **1998**, 987−988. (d) Tsuchiya, S. *J. Am. Chem. Soc.* **1999**, *121*, 48−53. (e) Otsuki, J.; Harada, K.; Araki, K. *Chem. Lett.* **1999**, 269−270. (f) Aiello, I.; Ghedini, M.; La Deda, M.; Pucci, D.; Francescangeli, O. *Eur. J. Inorg. Chem.* **1999**, 1367−1372. (g) Barigelletti, F.; Ghedini, M.; Pucci, D.; La Deda, M. *Chem. Lett.* **1999**, 297−298. (h) Miyaki, Y.; Onishi, T.; Kurosawa, H. *Chem. Lett.* **2000**, 1334−1335. (i) Yam, V. W. W.; Yang, Y.; Zhang, J.; Chu, B. W. K.; Zhu, N. *Organometallics* **2001**, *20*, 4911−4918. (j) Muraoka, T.; Kinbara, K.; Kobayashi, Y.; Aida, T. *J. Am. Chem. Soc.* **2003**, *125*, 5612−5613. (k) Horie, M.; Sakano, T.; Osakada, K.; Nakao, H. **2004**, *23*, 18−20.

10.1021/ic051184r CCC: $30.25
Published on Web 09/13/2005

Chart 1. Ferrocenylazobenzenes

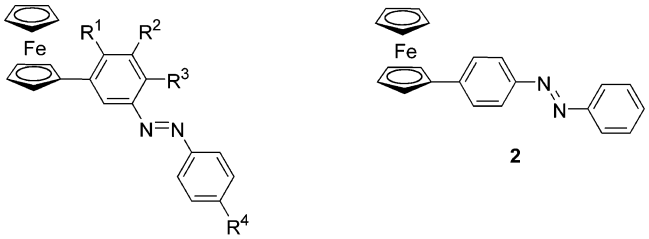

2

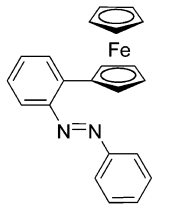

3

1: $R^1 = R^2 = R^3 = R^4 = H$
4: $R^1 = R^3 = R^4 = H$, R^2 = ferrocenyl
5: $R^1 = R^2 = R^4 = H$, $R^3 = Cl$
6: $R^1 = Cl$, $R^2 = R^3 = R^4 = H$
7: $R^1 = R^2 = R^4 = H$, $R^3 = CH_3$
8: $R^1 = R^2 = R^4 = H$, $R^3 = OH$
9: $R^1 = OH$, $R^2 = R^3 = R^4 = H$
10: $R^1 = R^2 = R^3 = H$, $R^4 = OSO_2C_6H_5CH_3$
11: $R^1 = R^2 = R^3 = H$, $R^4 = OH$
12: $R^1 = R^2 = R^3 = H$, $R^4 = O(CH_2)_8Br$
13: $R^1 = R^2 = R^3 = H$, $R^4 = O(CH_2)_8PO(OC_2H_5)_2$
14: $R^1 = R^2 = R^3 = H$, $R^4 = O(CH_2)_8S]_2$

benzene.[3l] 3-Ferrocenylazobenzene is especially interesting because it undergoes reversible isomerization not only with the usual UV light but also with green light. Since making this discovery, we have been investigating the effects of the degree of electronic interaction between azobenzene and ferrocene moieties on isomerization behavior by changing the position of ferrocenyl groups on azobenzene and introducing various substituents on the phenyl rings. In this paper, we describe in detail the isomerization behavior of ferrocenylazobenzenes, which can be controlled with photons, electrons, and protons.

Results and Discussion

Synthesis, Characterization, and X-ray Crystallographic Analysis. 3-Ferrocenylazobenzene (**1**) and 2-ferrocenylazobenzene (**3**) were prepared by a reaction of ferrocenylanilines and nitrosobenzene (see Chart 1). 4-Ferrocenylazobenzene (**2**) was prepared by a reaction of 4-aminoazobenzene and ferrocenium ions. 4′-substituted compounds of **1**, **5**−**10** were synthesized from 3-ferocenylaniline derivatives and nitrosobenzene or nitrosophenol *p*-toluenesulfonate (−OTs). The deprotection of the tosyl group of **10** was conducted by KOH to afford a phenol derivative, **11**, and the following Williamson's ether synthesis with 1,8-dibromooctane gave the bromo-terminated alkoxy derivative, **12**. Then, the bromo group-terminated alkyl chain was converted to phosphonic acid and disulfide diethyl ester to give **13** and **14**, respectively. 3,5-Diferrocenylazobenzene, **4**, was obtained through a reaction with boronic acid, and other derivatives were obtained by mixing 3-ferrocenylaniline derivatives with nitrosobenzene in acetic acid. These new compounds are highly stable in the air, and they are soluble in most relatively polar solvents, such as dichloromethane, chloroform, and acetonitrile. They were characterized by ^{1}H NMR and UV−vis spectra and by elemental analyses. The molecular structures of **1**, 2-chloro-5-ferrocenyl-azobenzene (**5**), and 3-ferrocenyl-4′-hydroxy-azobenzene (**11**) were determined by single-crystal X-ray crystallography.

The UV−vis absorption spectra of ferrocenylazobenzenes in acetonitrile or dichloromethane are shown in Figure 1, and the data are summarized in Table 1. Compounds **2** and **3**, in which the azo and ferrocene moieties are fully π-conjugated, showed a strong MLCT band at λ_{max} = 492 nm with molar extinction coefficient ϵ_{max} = 3690 $M^{-1}cm^{-1}$ and at λ_{max} = 478 nm with ϵ_{max} = 2190 $M^{-1}cm^{-1}$, respectively, in addition to an azo $\pi-\pi^*$ band at λ_{max} = 320 nm [nearly the same wavelength as that of azobenzene (317 nm)] and at λ_{max} = 352 nm, respectively. Compound **1** and its derivatives also exhibited a band around 390−492 nm ascribable to MLCT (or $\pi-\pi^*$) transitions (vide infra) in addition to an azo $\pi-\pi^*$ band at 319−352 nm, while the MLCT band intensity was lower than those of **2** and **3** because of the weaker electronic interaction between the azo and ferrocenyl groups. Substitution of an electron-donating group at the 4′ position of **1** caused a significant shift of the azobenzene moieties' $\pi-\pi^*$ bands to lower energy.

The molecular structures of **1**, **5**, and **11** were determined by single-crystal X-ray crystallography. The crystal data and refinement parameters are given in Table 2, and an ORTEP diagram of **1** is displayed in Figure 2 (ORTEP diagrams of **5** and **11** are shown in Figure S1 of the Supporting Information). The bond lengths of N1−N2 for **1**, **5**, and **11** are 1.257(2), 1.253(3), and 1.271(2) Å, respectively, and the dihedral angles between plane C6C7C8C9C10 and plane C11C12C13C14C15C16 are 16.540°, 24.524°, and 9.060°, respectively. The N1−N2 bond for **11** is longer than those for the others, but the length does not correlate well with the cis molar ratio in the photostationary state (PSS) upon green light irradiation (vide infra). On the other hand, the dihedral angle for **5** is larger than those for the others, and seems to correlate with the largest cis molar ratio in the PSS (vide infra). However, this result, which we attribute to the packing in crystals, does not affect the cis molar ratio because the single bond between ferrocene and azobenzene freely

(3) (a) Yutaka, T.; Kurihara, M.; Nishihara, H. *Mol. Cryst. Liq. Cryst.* **2000**, *343*, 193−198. (b) Yutaka, T.; Kurihara, M.; Kubo, K.; Nishihara, H. *Inorg. Chem.* **2000**, *39*, 3438−3439. (c) Nishihara, H. *Bull. Chem. Soc. Jpn.* **2001**, *74*, 19−29. (d) Yutaka, T.; Mori, I.; Kurihara, M.; Mizutani, J.; Kubo, K.; Furusho, S.; Matsumura, K.; Tamai, N.; Nishihara, H. *Inorg. Chem.* **2001**, *40*, 4986−4995. (e) Nihei, M.; Kurihara, M.; Mizutani, J.; Nishihara, H. *Chem. Lett.* **2001**, 852−853. (f) Nihei, M.; Kurihara, M.; Mizutani, J.; Nishihara, H. *J. Am. Chem. Soc.* **2003**, *125*, 2964−2973. (g) Kume, S.; Kurihara, M.; Nishihara, H. *Chem. Commun.* **2001**, 1656−1657. (h) Kume, S.; Kurihara, M.; Nishihara, H. *J. Kor. Electrochem. Soc.* **2002**, 189−191. (i) Kume, S.; Kurihara, M.; Nishihara, H. *Inorg. Chem.* **2003**, 42, 2194−2196. (j) Kurihara, M.; Nishihara, H. *Coord. Chem. Rev.* **2002**, *226*, 125−135. (k) Nishihara, H. *Macromol. Symp.* **2002**, *186*, 93−98. (l) Kurihara, M.; Hirooka, A.; Kume, S.; Sugimoto, M.; Nishihara, H. *J. Am. Chem. Soc.* **2002**, *124*, 8800−8801. (m) Yutaka, T.; Mori, I.; Kurihara, M.; Mizutani, J.; Tamai, N.; Kawai, T.; Irie, M.; Nishihara, H. *Inorg. Chem.* **2002**, *41*, 7143−7150. (n) Yutaka, T.; Mori, I.; Kurihara, M.; Tamai, N.; Nishihara, H. *Inorg. Chem.* **2003**, *42*, 6306−6313. (o) Nagashima, S.; Nihei, M.; Yamada, T.; Murata, M.; Kurihara, M.; Nishihara, H. *Macromol. Symp.* **2003** *204*, 93−101. (p) Kume, S.; Murata, M.; Ozeki, T.; Nishihara, H. *J. Am. Chem. Soc.* **2005**, *127*, 490−491. (q) Sakamoto, R.; Murata, M.; Kume, S.; Sampei, H.; Sugimoto, M.; Nishihara, H. *Chem. Commun.* **2005**, 1215−1217.

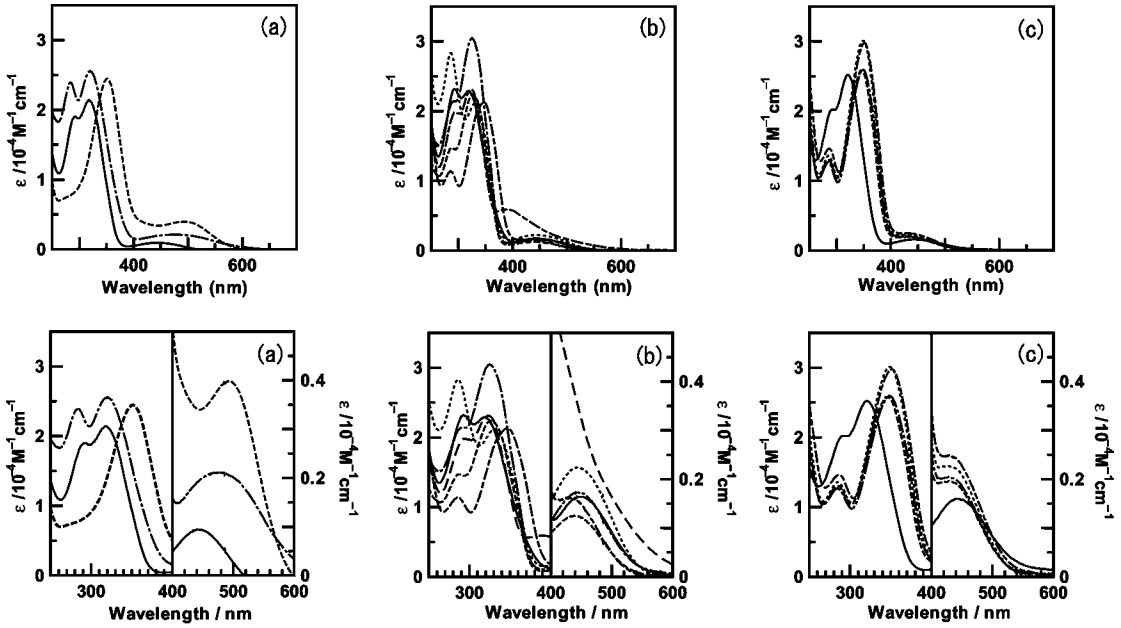

Figure 1. (a) Overlay plots of UV−vis spectra of ferrocenylazobenzene derivatives **1** (7.8×10^{-5} M, solid line), **2** (6.0×10^{-5} M, short-dashed line), and **3** (3.6×10^{-5} M, dotted-dashed line) in acetonitrile. (b) **1**-introduced substituents to the phenyl ring, which is bonded with ferrocene, **4** (3.6×10^{-5} M, solid line), **5** (4.6×10^{-5} M, short-dashed line), **6** (2.9×10^{-5} M, dotted-dashed line), **7** (6.1×10^{-5} M, dotted line), **8** (3.1×10^{-5} M, dashed-dashed line), and **9** (3.6×10^{-5} M, long-dashed) in acetonitrile. (c) 4′-substituted **1** derivatives **10** (3.0×10^{-5} M, solid line), **11** (3.0×10^{-5} M, short-dashed line), and **12** (2.8×10^{-5} M, dotted-dashed line) in acetonitrile and **13** (3.0×10^{-5} M, dotted line) and **14** (3.0×10^{-5} M, dashed-dashed line) in dichloromethane.

Table 1. UV−Vis Absorption Spectral Data of Ferrocenylazobenzene Derivatives

	$\lambda_{max,1}$ (nm)	$\epsilon_{max,1}$ ($M^{-1}\,cm^{-1}$)	$\lambda_{max,2}$ (nm)	$\epsilon_{max,2}$ ($M^{-1}\,cm^{-1}$)
1	319	21 400	444	1851
2	352	24 500	492	3677
3	320	25 900	478	2190
4	331	21 100	446	22698
5	319	22 900	448	1512
6	325	30 500	444	1432
7	326	22 400	440	1235
8	324	23 100	390	5915
9	347	21 100	451	5038
10	320	25 200	440	1600
11	346	25 800	428	1969
12	348	26 000	430	2050
13	352	29 800	429	2493
14	348	30 100	420	2271

rotates in solution. It should be noted that there are no hydrogen bonds between hydroxyl groups in the crystal of **11**.

Photon-, Electron-, and Proton-Coupled Isomerization Behavior of 1. Figure 3 shows the spectral change of **1** in acetonitrile by photoirradiation. A decrease in the intensity of the $\pi-\pi^*$ band, derived mainly from the azo moiety, was observed with isosbestic points at 270 and 395 nm through UV (313 nm) irradiation, whose wavelength corresponds to the maximum in the $\pi-\pi^*$ band. The same spectral change was observed through green (546 nm) irradiation, whose wavelength corresponds to the edge of the visible band. Subsequent irradiation with blue light (436 nm) recovered the intensity of the azo $\pi-\pi^*$ band. This spectroscopic behavior is characteristic of the reversible trans-to-cis isomerization of azobenzene, indicating that the trans-to-cis photoisomerization of **1** proceeds not only through UV but also through green irradiation. It is expected that an MLCT character plays an important role in isomerization with green light (vide infra). Organic azobenzenes also have the ability to shift the $\pi-\pi^*$ absorption wavelength up to around 500 nm by the introduction of donor and acceptor units, so-called push−pull azobenzenes, but such azobenzenes generally have very short half-lives, owing to the low stability of the cis form.[4] In contrast, the photogenerated cis form of **1** has a high stability for thermal cis-to-trans isomerization. The rate constant for the thermal cis-to-trans isomerization of **1** was estimated to be $1.3 \times 10^{-4}\ s^{-1}$ at 70 °C, consistent with that of azobenzene ($k = 1.3 \times 10^{-4}\ s^{-1}$ at 70 °C).

The ^{1}H NMR signals of **1** were shifted to upper-field positions after UV and green light irradiation (Figure S2, Supporting Information), indicating the generation of the cis form.[3d,5] The cis molar ratio of **1** in the PSS, estimated from the integral ratio of the ^{1}H NMR signals of the ferrocenyl moiety, was 35% upon green light (546 nm) irradiation, and the PSS was changed into a more cis-rich state (61% cis molar ratio) upon UV (313 nm) irradiation. The quantum yield for the trans-to-cis photoisomerization of **1** was estimated to be 0.021 for UV (313 nm) irradiation, which is smaller than that of azobenzene [$\Phi_{t\to c} = 0.12$ (313 nm excitation)],[6] and a much higher value, 0.51, was obtained for green light (546 nm) irradiation. The PSS reached a more trans-rich state (17% cis molar ratio) upon blue light (436 nm) irradiation, which effectively generates the $n-\pi^*$ excitation state of the cis form.

(4) (a) Rau, H. *Photochromic Molecules and Systems*; Elsevier: Amsterdam, 1990; Chapter 4. (b) Nishimura, N.; Kosako, S.; Sueishi, Y. *Bull. Chem. Soc. Jpn.* **1984**, *57*, 1617−1625. (c) Nishimura, N.; Sueyoshi, T.; Yamanaka, H.; Imai, E.; Yamamoto, S.; Hasegawa, S. *Bull. Chem. Soc. Jpn.* **1976**, *49*, 1381−1387. (d) Sueyoshi, T.; Nishimura, N.; Yamamoto, S.; Hasegawa, S. *Chem. Lett.* **1974**, 1131−1134.
(5) Rudolph-Böhner, S.; Kruger, M.; Oesterhelt, D.; Moroder, L.; Nägel, T.; Wachtveitl, J. *J. Photochem. Photobiol., A* **1997**, *105*, 235−248.
(6) Rau, H. *J. Photochem.* **1984**, *26*, 221−225.

Table 2. Crystal Data and Refinement Parameters for **1**, **5**, and **11**

	1	**5**	**11**
empirical formula	$C_{22}H_{18}FeN_2$	$C_{22}H_{17}ClFeN_2$	$C_{22}H_{19}FeN_2O$
fw	366.24	400.69	382.24
cryst dimensions	0.20× 0.20 × 0.20 mm	0.40 × 0.20 × 0.10 mm	0.40 × 0.30 × 0.10 mm
cryst syst	monoclinic	monoclinic	orthorhombic
lattice params	a = 11.157(11) Å	a = 10.61(1) Å	a = 25.55(2) Å
	b = 7.528(7) Å	b = 7.825(10) Å	b = 11.318(7) Å
	c = 20.34(2) Å	c = 21.57(3) Å	c = 5.848(4) Å
	β = 96.805(12)°	β = 92.808(8)°	
	V = 1696.3(28) Å^3	V = 1788.3(39) Å^3	V = 1690.9(18) Å^3
space group	$P2_1/c$ (#14)	$P2_1/c$ (#14)	$Pna2_1$ (#33)
Z value	4	4	4
μ (Mo Kα)	8.94 cm^{-1}	9.99 cm^{-1}	9.04 cm^{-1}
D (calcd)	1.434 g/cm^3	1.488 g/cm^3	1.501 g/cm^3
F_{000}	760	824	792
R_1[a]	0.047	0.042	0.041
wR_2[b]	0.090	0.099	0.092
GOF[c]	1.115	1.112	1.000

[a] $R_1 = \sum||F_o| - |F_c||/\sum|F_o|$. [b] $wR_2 = \{\sum[w(F_o^2 - F_c^2)^2]/\sum w(F_o^2)^2]\}^{1/2}$. [c] GOF = $\{\sum[w(F_o^2 - F_c^2)^2]/\sum(N_o - N_v)^2]\}^{1/2}$, where N_o = number of observations and N_v = number of variables.

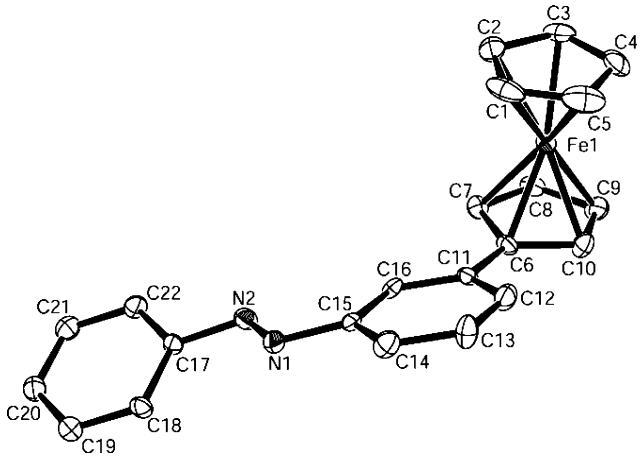

Figure 2. ORTEP diagram of **1** with 50% probability. Hydrogen atoms are omitted for clarity. Selected bond lengths (Å), dihedral angles (deg), and torsion angles (deg) are as follows: N(1)−N(2) 1.2572, N(1)−C(15) 1.4306, N(2)−C(17) 1.4295, C(11)−C(6) 1.4774, Fe(1)−C(6) 2.0353, C(6−10)−C(11−16) 16.540, C(15)−N(1)−N(2)−C(17) 175.0(2).

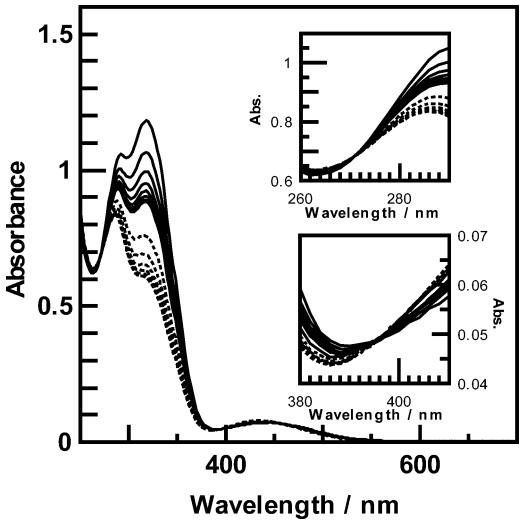

Figure 3. UV−vis absorption spectral change of **1** (5.5×10^{-5} M) in acetonitrile upon photoirradiation with a monochromatic light at 546 nm (solid lines) for 21 min and subsequent irradiation with a monochromatic light at 320 nm (dotted lines) for 4 min. Inset shows the spectral changes around the isosbestic points.

A cyclic voltammogram of *trans*-**1** in 0.1 M *n*-Bu_4NClO_4−acetonitrile solution exhibited a reversible oxidation wave due to Fe^{III}/Fe^{II} at $E^{0'}$ = 0.059 V versus Fc^+/Fc (Figure S3, Supporting Information). The sample solution was photoirradiated to generate a trans−cis mixture (35% cis molar ratio), the oxidation potential of which was determined to be 0.054 V versus Fc^+/Fc (Figure S3), indicating that the isomerization caused no significant shift in the redox potential.

The electrochemical oxidation of *trans*-**1** in 0.1 M *n*-Bu_4NClO_4−acetonitrile from the ferrocene to the ferrocenium state was realized upon controlled-potential electrolysis at 0.45 V versus Ag/Ag^+. Upon oxidation, an absorption spectral change of the compound was observed. Namely, the $\pi-\pi^*$ band shifted to higher energy from λ_{max} = 319 to 311 nm, an MLCT band around 500 nm decreased, and a weak LMCT band appeared at 730 nm (Figure S4a, Supporting Information).[7] Subsequent controlled-potential electrolysis at −0.1 V versus Ag/Ag^+ recovered the initial absorption spectrum (Figure S4b), indicating the high reversibility of this redox reaction. The chemical oxidation of *trans*-**1** with $[Fe(\eta^5\text{-}C_5H_4Cl)_2]PF_6$ [8] was also realized, and it gave the same spectroscopic behavior as was observed upon electrochemical oxidation.

The trans-to-cis photoisomerization behavior in the ferrocenium state was much different from that in the ferrocene state. UV light irradiation of *trans*-$\mathbf{1}^+$ (Fe^{III} state) in acetonitrile caused a decrease in the $\pi-\pi^*$ band intensity, indicating trans-to-cis isomerization, whereas almost no spectral change was observed upon exposure to green light. Photoirradiation to a newly appearing LMCT band did not cause any photoreaction. These results indicate that the drastic change in the response to green light is caused by the elimination of an MLCT band upon oxidation of the

(7) Kurosawa, M.; Nankawa, T.; Matsuda, T.; Kubo, K.; Kurihara, M.; Nishihara, H. *Inorg. Chem.* **1999**, *38*, 5113−5123.

(8) Horikoshi, T.; Kubo, K.; Nishihara, H. *J. Chem. Soc., Dalton Trans.* **1999**, 3355−3360.

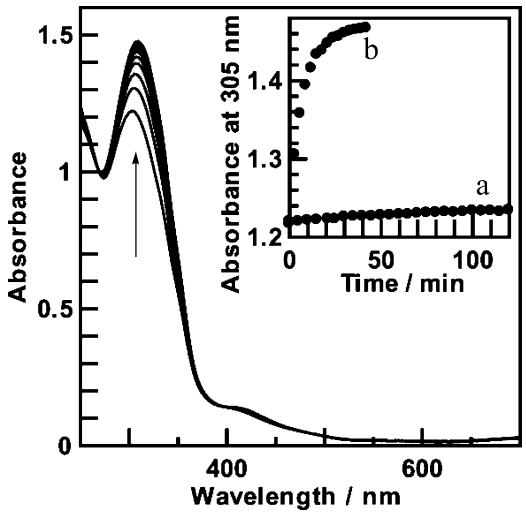

Figure 4. UV−vis absorption spectral change of the following sample solution upon photoirradiation with a monochromatic light at 546 nm; (inset) time course change in absorbance at 305 nm of the sample solution in the dark (a) or upon photoirradiation with a monochromatic light at 546 nm (b). The sample solution was prepared by photoirradiation with a monochromatic light at 546 nm to 3-ferrocenylazobenzene in acetonitrile (5.62×10^{-5} M) to reach a photostationary state followed by oxidation with 1 equiv of 1,1′-dichloroferrocenium hexafluorophosphate.

metal center and that the MLCT character plays an important role in isomerization with green light in the ferrocene state. The cis-to-trans thermal isomerization rate in the ferrocenium state estimated by UV−vis spectral change was 8.7×10^{-4} s^{-1} at 70 °C (Figure 4).

It is expected that the MLCT character makes no contribution to the ferrocenium state, and thus, cis-to-trans isomerization through the $n-\pi^*$ excitation state proceeds mainly upon green light irradiation, achieving a very trans-rich state with green light irradiation in the PSS. The large difference in the cis molar ratio in the PSS between the Fe^{II} and Fe^{III} states suggests the possibility of reversible trans-to-cis conversion upon irradiation with a single green light by changing the oxidation state of the iron center. The following experiments proved this possibility. An acetonitrile solution of *trans*-**1** of Fe^{II} was irradiated with green light (546 nm) to reach the PSS (35% cis molar ratio), and the resulting mixture of trans and cis forms was oxidized to the Fe^{III} state immediately after a stoichiometric amount of $[Fe(\eta^5\text{-}C_5H_4Cl)_2]PF_6$ was added. After the oxidation, the recovery of the $\pi-\pi^*$ band absorbance was not pronounced in intensity after several hours in the dark at room temperature, and the thermal isomerization to the trans form proceeded very slowly in the Fe^{III} state, as noted above. Green light irradiation promoted the increase in absorbance, which reached the trans-rich PSS characteristic of the ferrocenium state, suggesting that almost all of the trans form was recovered (Figure 4). These results indicate that reversible trans-to-cis isomerization can be achieved by a combination of "on−off switching" of the MLCT character due to the Fe^{III}/Fe^{II} redox change and irradiation with a single green light source (Scheme 1).

The protonation behavior of **1** was investigated. When 1 equiv of CF_3SO_3H was added to an acetonitrile solution of **1**, the UV−vis absorption spectrum changed within a few minutes; the azo $\pi-\pi^*$ band was slightly blue-shifted, the intensity of the visible band was increased, and a new band appeared around 730 nm (Figure S5, Supporting Information). Although there is a report investigating the spectral behavior of ferrocenylazobenzenes in acidic solutions,[9] to our knowledge, there are no reports that the stoichiometric amount of acid completely changes the absorption spectra of ferrocenylazobenzenes. We have not isolated and characterized the product, but its structure is likely to be one in which the azo nitrogen is protonated, judging from the protonation reaction of azobenzene-conjugated metalladithiolenes.[3f,3g] The cis form of **1** is changed into the trans form, which is catalyzed by a small amount of CF_3SO_3H (Scheme 1; Figure S6, Supporting Information). The rate constant for the cis-to-trans isomerization of **1** after the addition of 0.08 equiv of CF_3SO_3H was estimated to be 4.8×10^{-2} s^{-1} at 20 °C.

Isomerization Behavior of 2. The photochemical behavior of **2** is much different from that of **1**. In the UV−vis spectra of **2** in acetonitrile, a decrease in the azo $\pi-\pi^*$ band intensity of this sample solution was observed with an isosbestic point at 304 nm through UV light (365 nm) irradiation (Figure 5a). Subsequent blue light (436 nm) irradiation, which may excite the azo $n-\pi^*$ band of the cis form, recovered the azo $\pi-\pi^*$ band intensity (Figure 5b), indicating reversible trans−cis photoisomerization of the azobenzene moiety. A decrease in the azo $\pi-\pi^*$ band intensity was also observed through green light (546 nm) irradiation to a low-lying MLCT band, as in the case of **1**, but the absorption spectrum of the resulting sample solution was only slightly different from that of the trans form. The photogenerated cis form has a relatively high stability for thermal cis-to-trans isomerization, and the rate constant for the thermal cis-to-trans isomerization of **2** was estimated to be 1.2×10^{-3} s^{-1} at 70 °C, an order of magnitude higher than that of azobenzene or **1**. The cis molar ratios of **2** in the PSS upon UV light (365 nm) and green light (546 nm) irradiation were 42% and 6%, respectively, which were estimated from the integral ratio of ^1H NMR signals of the ferrocenyl moiety (Figure S7, Supporting Information). The quantum yield for the trans-to-cis photoisomerization, $\Phi_{t\rightarrow c}$, of **2** was estimated to be 0.0033, which is smaller than that of **1**, for UV light (365 nm) irradiation.

The reversible redox reaction of the Fe^{III}/Fe^{II} couple of *trans*-**2** occurs at $E^{0'} = 0.16$ V versus Ag/Ag^+ in 0.1 M *n*-Bu_4NClO_4−acetonitrile solution. Electrochemical oxidation caused an absorption spectral change in which the $\pi-\pi^*$ band shifted to higher energy from $\lambda_{max} = 352$ to 338 nm; an MLCT band around 500 nm decreased, and a weak LMCT band appeared at 769 nm (Figure S8, Supporting Information).

When the oxidizing agent, $[Fe(\eta^5\text{-}C_5H_4Cl)_2]PF_6$, was added to the acetonitrile solution of the photogenerated trans−cis mixture of **2** at room temperature, the observed absorption spectrum was the same as that of the trans form. This result

(9) Little, W. F.; Berry, R. A.; Kannan, P. *J. Am. Chem. Soc.* **1962**, *84*, 2525−2529.

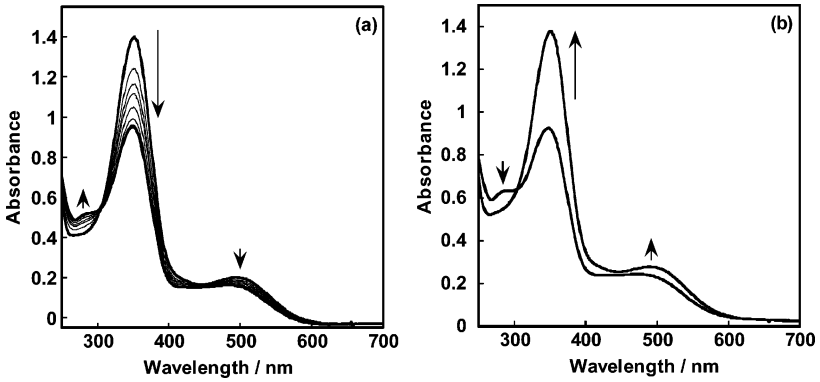

Figure 5. (a) UV−vis absorption spectral change of **2** (5.46×10^{-5} M) in acetonitrile upon photoirradiation with a monochromatic light at 365 nm for 14 min and (b) subsequent irradiation with a monochromatic light at 405 nm.

Scheme 1. Redox- and Proton-Conjugated Photoisomerization Pathway

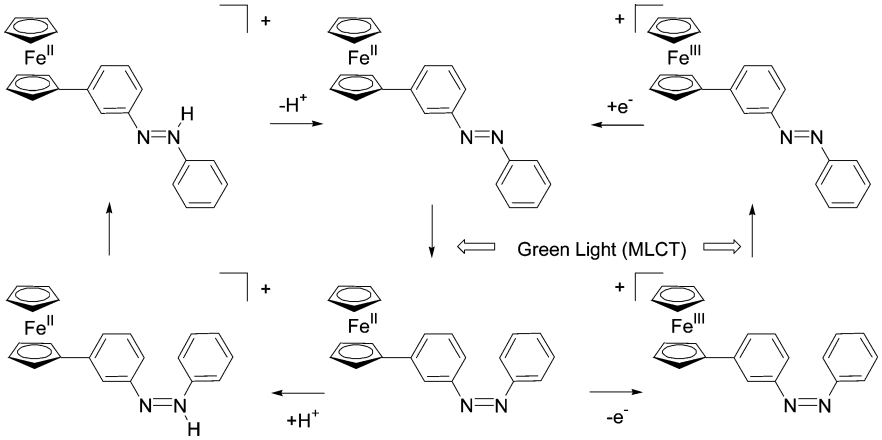

Scheme 2. Resonance Structures of **2**

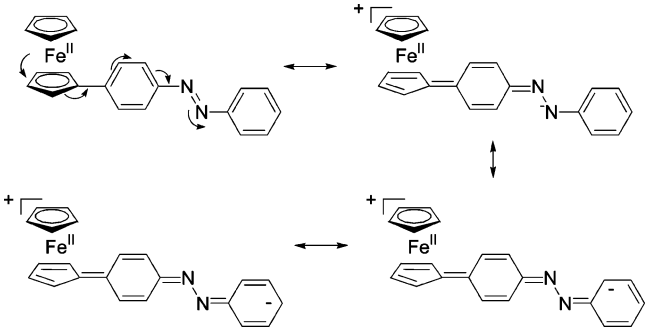

implies very fast cis-to-trans thermal isomerization in the ferrocenium state. When chemical oxidation was carried out at 5 °C, the absorption spectra of the cis−trans mixture changed, and the rate constant of this change was estimated to be 3.8×10^{-3} s^{-1}. The low stability of *cis*-$\mathbf{2}^+$ (Fe^{III} state) is attributed to the large delocalization of electrons on the conjugated ligand, causing a canonical conformation with a η^6-fulvene-type structure[10] and decreasing the double-bond character of N═N (Scheme 2). This is reasonable because the cis form of **1** in the ferrocenium state, which cannot give a canonical structure, has a higher thermal stability than **2**, as noted above.

The protonation behavior of **2** was also examined. An acetonitrile solution of **2** showed a UV−vis absorption spectral change upon the addition of 1.1 equiv of CF_3SO_3H. Immediately after the addition of CF_3SO_3H, the absorbance around 500 nm was increased in intensity and a new band appeared around 800 nm (Figure S9, Supporting Information), probably forming the monoprotonated form, as was the case for **1**. Proton-catalyzed cis-to-trans isomerization was also observed. The rate constant for cis-to-trans isomerization after the addition of 0.08 equiv of CF_3SO_3H was estimated to be 1.4×10^{-2} s^{-1} at 20 °C (Figure S10, Supporting Information).

Isomerization Behavior of 3. Another geometric isomer in the ferrocenylazobenzene family, **3**, was also employed for the isomerization study. The absorption spectral change of **3** in acetonitrile was observed upon UV light irradiation (313 nm; Figure S11, Supporting Information), but the decrease in intensity of the $\pi-\pi^*$ band was extremely small. Subsequent violet light irradiation (405 nm) caused a back reaction. Green light irradiation (546 nm) to the MLCT band also caused trans-to-cis isomerization, though only to a small extent. The cis molar ratios in the PSS upon UV light (313 nm) and green light (546 nm) irradiation were estimated to be 5% and 7%, respectively, judging from the integral ratio of the ^1H NMR signal (Figure S12, Supporting Information).

Excited-State Calculations of 1 and 2. It is of interest to understand why green light irradiation caused a much

(10) (a) Murata, M.; Fujita, T.; Yamada, M.; Kurihara, M.; Nishihara, H. *Chem. Lett.* **2000**, 1328−1329. (b) Murata, M.; Yamada, M.; Fujita, T.; Kojima, K.; Kurihara, M.; Kubo, K.; Kobayashi, Y.; Nishihara, H. *J. Am. Chem. Soc.* **2001**, *123*, 12903−12904.

Table 3. Experimental and Theoretical[a] Excitation Energies to the Lowest Excited State among Those of Similar Character

excitation energy/eV			
exptl	theor	oscillator strength (theor)	assignment (CI coefficient)[b]
		trans-**1**	
	2.43	0.001	63[c] → 67 (0.55)
			65 → 67 (−0.33)
2.79	3.02	0.060	64 → 67 (0.65)
			62 → 67 (0.19)
3.90	3.49	0.693	62 → 67 (0.59)
		cis-**1**	
	2.45	0.047	64 → 67 (0.56)
			63 → 67 (−0.21)
	3.16	0.001	62 → 68 (0.35)
			63 → 67 (0.31)
	3.96	0.103	58 → 67 (0.58)
		trans-**2**	
	2.42	<0.001	63 → 67 (0.66)
2.51	2.63	0.113	66 → 67 (0.57)
			66 → 68 (0.22)
			61 → 68 (−0.23)
3.52	3.03	0.752	64 → 67 (0.55)

[a] TD-DFT calculations with three-parametrized Becke−Lee−Yang−Parr (B3LYP) hybrid exchange-correlation functional. [b] The expansion coefficient for the excited-state wave function. [c] The numbers of molecular orbitals refer to those displayed in Figure 6.

higher cis molar ratio in **1** than it did in **2**. Time-dependent density functional theory (TD-DFT) calculations for **1** in the trans and cis forms and for **2** in the trans form were carried out to investigate the singlet excited state in which the isomerization occurs. The calculated excitation energies in the trans form were in reasonable agreement with the experimental values, and the observed trends in the experimental absorption spectra were correctly reproduced (Table 3). The noticeable features in the nature of the *trans*-**1** excited states are that the azo $n-\pi^*$ strongly mixes with the MLCT configuration and that the ground state orbital for the 3.02 eV MLCT state (number 64) is delocalized over Fe and the Cp ring rather than localized on the iron (Figure 6). The presence of the MLCT character is the reason the molar extinction coefficient of the visible band ($\lambda_{max} = 444$ nm, $\epsilon = 1.86 \times 10^3$ M^{-1} cm^{-1}) is much larger than that of the $n-\pi^*$ band of *trans*-azobenzene ($\lambda_{max} = 444$ nm, $\epsilon = 5.15 \times 10^2$ M^{-1} cm^{-1}). The origin of the visible band in **1** is different from that of **2**, because the ground state orbital for the 2.51 eV MLCT state of the latter is localized on the iron (Figure 6). It seems that isomerization through the "pure" MLCT excitation state barely proceeds; the initial orbital of the MLCT of **1** (number 66) is not a pure metal-based d orbital, but the ligand character, as in the azobenzene moiety, is mixed. It is possible that the green-irradiation-induced trans-to-cis isomerization of **1** occurs on the potential energy surface for the MLCT excited state. In fact, the almost complete absence of a response to green light for the cis formation in the ferrocenium state is caused by the disappearance of the MLCT character in the ferrocene state upon oxidation to the ferrocenium state. The appearance of a $n-\pi^*$ band at 2.45 eV for *cis*-**1** in the calculation (see Table 3) supports the idea that the cis-to-trans isomerization of **1** in the oxidized form with green light occurs through the $n-\pi^*$ excited state.

Photoisomerization Behaviors of Derivatives of 1. Among the three geometric isomers of ferrocenylazobenzene, **1** exhibits the most significant isomerization behavior in response to green light. But the cis molar ratio obtained through green light irradiation was moderate, 35%. To improve the cis molar ratio in the PSS, we examined the effects of electron-withdrawing and -donating substituents on two phenyl rings. The results are summarized in Table 4.

As for the derivatives (**12**, **13**, **14**) in which an electron-donating group is introduced at the 4′ position, the cis molar ratio at 365 nm irradiation was higher than it was with **1**, but that at 546 nm irradiation was lower than that with **1**. In contrast, the electron-withdrawing $-OSO_2C_6H_4CH_3$ group at the 4′ position did not affect the cis molar ratio significantly. It should be noted that the OH-substituted derivative, **11**, exhibited no spectral changes by irradiation with either UV or visible light. It has been reported that the cis-to-trans isomerization of hydoxyazo compounds was extremely fast in polar solvents, because the tautomerism of azo and hydrazone structures lowers the activation energy.[4,11,12]

When the ortho position to the ferrocenyl group was substituted with an electron-donating methyl group (**7**) or an electron-withdrawing chloro group (**6**), the UV and green light photoisomerization behaviors were similar to those of **1**. In contrast, when the para position to the ferrocenyl group was substituted with the chloro group (**5**), the highest value of the cis molar ratio at 546 nm was attained. As the difference in energies between $\pi-\pi^*$ and MLCT bands ($\nu_{max1} - \nu_{max2}$ in Table 3) is largest for **5** among all the derivatives in this study, we assume that the $n-\pi^*$ and MLCT bands are less overlapped, provided that the energies of the $\pi-\pi^*$ and $n-\pi^*$ bands are shifted in parallel. Consequently, the trans-to-cis isomerization promoted by the MLCT excitation is least perturbed by the cis-to-trans isomerization by the $n-\pi^*$ excitation.

A derivative with two ferrocenyl moieties, **4**, was also employed. The intensity of the MLCT band was greater than that with **1** (the molar extinction coefficient at 446 nm, ϵ_{446}, is 2698 for **4**, whereas $\epsilon_{444} = 1851$ for **1**), but the cis molar ratio in the PSS upon green light irradiation (546 nm) was 29%, which was not improved compared to that of **1**. This is probably because the $\pi-\pi^*$ band shifted to a longer wavelength, and accordingly, the $n-\pi^*$ band shifted in the same direction and overlapped more effectively with the MLCT band.

Conclusion

3-Ferrocenylazobenzene, **1**, showed reversible photoisomerization with UV and blue light irradiation. Excitation of the MLCT band by green light irradiation also caused

(11) Hartley, G. S. *J. Chem. Soc.* **1938**, 633−642.
(12) Brode, W. R.; Gould, J. H.; Wyman, G. M. *J. Am. Chem. Soc.* **1952**, *74*, 4641−4646.

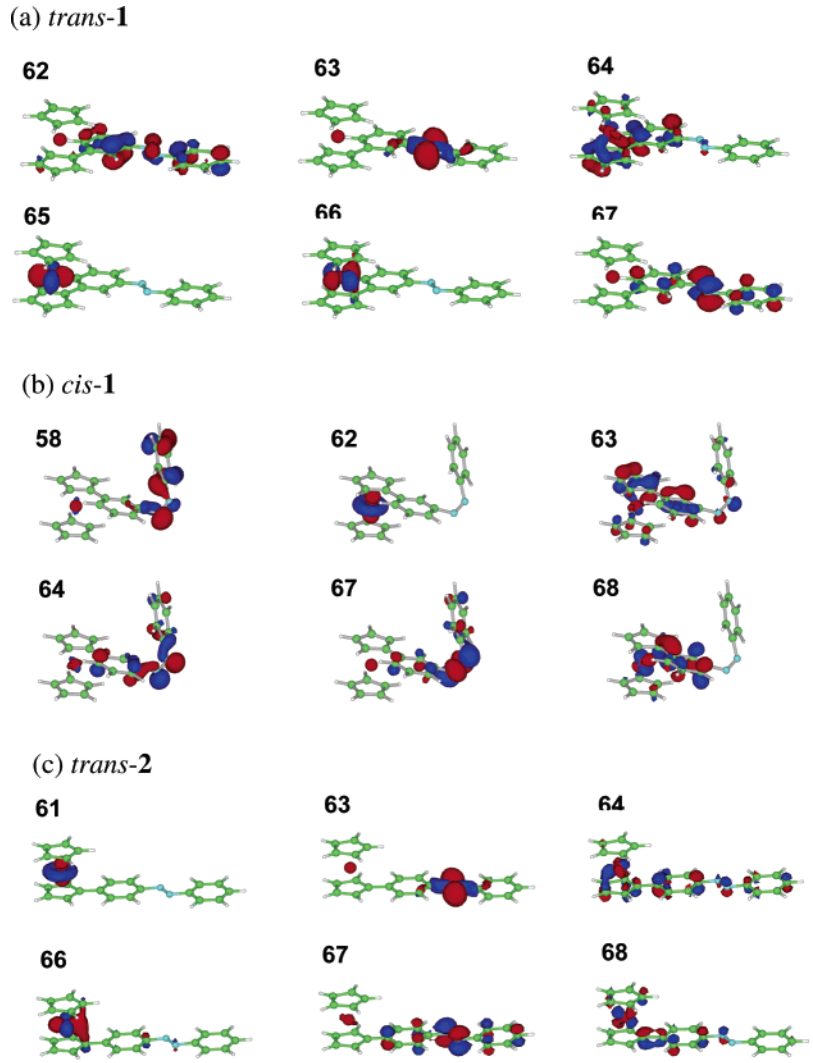

Figure 6. The molecular orbitals contributing to the main UV−vis absorption bands of (a) *trans*-**1**, (b) *cis*-**1**, and (c) *trans*-**2**.

Table 4. cis Molar Ratios[a] of Ferrocenylazobenzene Derivatives in the PSS on Monochromatic Light Irradiation

	excitation wavelength/nm			
	313	365	436	546
1	61 (45)%		17%	35 (26)%
2		42%		6%
3	5%			7%
4	35%		(7)%	29 (17)%
5	39 (38)%		16 (15)%	47 (36)%
6	56 (50)%		15 (13)%	22 (19)%
7	67 (52)%		19 (16)%	20 (17)%
8		∼0%	∼0%	∼0%
9		∼0%	∼0%	∼0%
10	(48)%			(18)%
11		(∼0)%	(∼0)%	(∼0)%
12		(68)%	(22)%	(8)%
13		(77)%	(22)%	(9)%
14		(81)%	(35)%	(2)%

[a] The cis molar ratios were obtained from the integral ratio of ^{1}H NMR signals of the ferrocenyl moiety. The numbers in parentheses were obtained using UV−vis spectral changes.

trans-to-cis photoisomerization. Only trans-to-cis efficient isomerization with MLCT excitation was observed for the case of **1**. The response to green light was altered by switching the oxidation state of the ferrocenyl moiety, which controls the existence of an MLCT band. The different responses to green light between the Fe(II) and Fe(III) states allowed us to realize redox-conjugated reversible isomerization with a single green light source. Compound **1** has a large affinity to protons, and cis-to-trans isomerization was accelerated by a small amount of TfOH. A variety of responses to external perturbations such as photons, redox, and protons created a multimodal isomerization route with a combination of those responses.

4-Ferrocenylazobenzene, **2**, showed reversible trans−cis photoisomerization with UV and visible light irradiation. The cis form of **2** has a high stability in the Fe(II) state, and its thermal stability was controlled by an oxidation state of the metal center, which affected the electronic state of the azo moiety through the conjugated chain. In the Fe(III) state, the rate constant for thermal cis-to-trans isomerization was drastically larger than that in the Fe(II) state. The azo moiety of **2** also showed a large affinity to protons because of the strong electron-donating ability of the ferrocenyl moiety. A proton-coupled cis-to-trans isomerization route was constructed for **2**. 2-Ferrocenylazobenzene, **3**, underwent reversible photoisomerization with UV and visible light irradiation, but the amount of the cis form photogenerated was extremely

small. The introduction of an electron-withdrawing substituent to **1** improved the efficiency of photoisomerization with green light.

Experimental Section

Materials. Ferrocene was purchased from Kanto Chemicals and recrystallized from hexane before use. 1,8-Dibromooctane was purchased from Aldrich. 2-Methyl-5-nitroaniline, 4-chloro-3-nitroaniline, 2-chloro-5-nitroaniline, 4-nitro-2-aminophenol, 2-nitro-4-aminophenol, 2,6-dibromo-4-nitroaniline, and dichlorobis(triphenylphosphine)palladium(II) were purchased from Tokyo Kasei Kogyo and used as received. Sodium nitrite and nitrobenzene were purchased from Wako Pure Chemical Industries and used as received. Zinc powder was purchased from Koso Chemical, washed with hydrochloric acid, and then evaporated before use. Tin powder was purchased from Koso Chemical and used as received. Other reagents and solvents were purchased from Kanto Chemicals and used as received. Spectroscopic-grade acetonitrile (Aldrich) and spectroscopic-grade dichloromethane (Kanto Chemicals) were used for UV−vis absorption spectroscopy. The acetonitrile used for the electrochemical measurements was of HPLC grade (Kanto Chemicals). *n*-Tetrabutylammonium perchlorate (lithium battery grade) was purchased from Tomiyama Chemical and recrystallized from HPLC-grade ethanol before use. 3-Ferrocenylnitrobenzene (**a1**),[13−15] 2-ferrocenylnitrobenzene (**a3**),[14,16−18] 3,5-diferrocenylnitrobenzene (**a4**),[19] 2-ferrocenyl-4-nitrotoluene (**a7**),[20] ferrocenylboronic acid,[21] 3,5-dibromonitrobenzene,[19] 3-ferrocenylaniline (**b1**),[5,20] 2-ferrocenylaniline (**b3**),[18] 3,5-di-ferrocenylaniline (**b4**),[15] nitrosobenzene,[22] and 1,1′-dichloroferrocenium hexafluorophosphate[23,24] were prepared according to the methods in the literature.

Apparatus. UV−vis absorption spectra were obtained on an 8453 UV−visible Spectroscopy System (Hewlett-Packard) or a V-570 spectrophotomer (Jasco). ^{1}H NMR spectra were obtained on an EX270 or JNM-AL400 spectrometer (both by JEOL). Photoirradiation experiments were carried out using a Ushio 500W super-high-pressure mercury lamp, the USH-500D, as a light source. The monochromatic light was provided by a JASCO CT-10T monochromator.

Ferrocenylnitrobenzene Derivatives. (Scheme S1A, Supporting Information, illustrates the synthesis of new ferrocenylazobenzenes.) 2-Ferrocenyl-5-chloronitrobenzene (**a5**) was prepared according to a report on the synthesis of 3-ferrocenylnitrobenzene (**a1**).[13−15] Ferrocene (4.00 g, 21.5 mmol) was added to sulfuric acid (15 mL). The resulting deep blue ferrocenium solution was stirred at room temperature for 2 h, then poured into water (100 mL) cooled on an ice bath. A solution of sodium nitrite (1.06 g, 15.4 mmol) in water at 0 °C was added dropwise with stirring to a solution of 2-chloro-5-nitroaniline (2.50 g, 14.5 mmol) in 1:1 water/hydrochloric acid (10 mL) kept at 0 °C by an ice bath, and the mixture was stirred for 30 min to ensure complete diazotization. The diazonium solution was added to a ferrocenium solution at 0 °C with vigorous stirring. Then, copper powder (1.00 g) was added to the solution as a catalyst and allowed to warm to room temperature. After 24 h of stirring, the nitrogen effervescence ceased, and ascorbic acid (5.00 g) was added to reduce the unreacted ferrocenium to ferrocene. Dichloromethane was added, and the solution was filtered through Celite. The organic layer was separated, and the aqueous layer was extracted with dichloromethane. The combined organic extracts were dried over sodium sulfate and filtered, and the solvent was removed. The dark solid was purified by column chromatography with an increasing proportion of dichloromethane in hexane as an eluent. The first yellow-orange band was eluted with pure hexane and yielded unchanged ferrocene. The second band, eluted with 50% dichloromethane/hexane, was collected. Removal of the solvent, followed by recrystallization from dichloromethane/hexane, afforded **a5**. Yield: 32% (1.61 g, 4.7 mmol). ^{1}H NMR (270 MHz, $CDCl_3$): δ 7.91 (d, $J = 2.2$ Hz, 1H, C_6H_3), 7.57 (dd, $J = 8.1$ Hz, $J = 2.2$ Hz, 1H, C_6H_3), 7.43 (d, $J = 8.1$ Hz, C_6H_3), 4.66 (t, $J = 1.9$ Hz, 2H, C_5H_4), 4.42 (t, $J = 1.9$ Hz, 2H, C_5H_4), 4.07 (s, 5H, C_5H_5).

In the same way, 4-chloro-3-ferrocenylnitrobenzene (**a6**), 4-ferrocenyl-2-nitrophenol (**a8**), and 2-ferrocenyl-4-nitrophenol (**a9**) were prepared in 20% yield (1.24 g) from 4-chloro-3-nitroaniline (2.42 g, 14.0 mmol), 36% yield (1.54 g) from 2-nitro-4-aminophenol (2.06 g, 13.4 mmol), and 22% yield (0.99 g) from 2-amino-4-nitrophenol (2.17 g, 14.1 mmol), respectively. *Data for **a6***. ^{1}H NMR (400 MHz, $CDCl_3$): δ 8.51 (d, $J = 2.68$ Hz, 1H, C_6H_3), 7.97 (dd, $J = 8.9$ Hz, $J = 2.81$ Hz, 1H, C_6H_3), 7.49 (d, $J = 8.78$ Hz, C_6H_3), 4.83 (s, 2H, C_5H_4), 4.44 (s, 2H, C_5H_4), 4.18 (s, 5H, C_5H_5). *Data for **a8***. ^{1}H NMR (270 MHz, $CDCl_3$): δ 10.53 (s, 1H, OH), 8.13 (d, $J = 2.1$ Hz, 1H, C_6H_3), 7.71 (dd, $J = 8.9$ Hz, $J = 2.1$ Hz, 1H, C_6H_3), 7.11 (d, $J = 8.9$ Hz, 1H, C_6H_3), 4.62 (t, $J = 1.9$ Hz, 2H, C_5H_4), 4.36 (t, $J = 1.9$ Hz, 2H, C_5H_4), 4.06 (s, 5H, C_5H_5). *Data for **a9***. ^{1}H NMR (270 MHz, $CDCl_3$): δ 8.14, 8.10, 8.01 (s, 1H, OH), 7.03 (d, $J = 8.1$ Hz), 4.57 (t, $J = 1.6$ Hz, 2H, C_5H_4), 4.51 (t, $J = 1.6$ Hz, 2H, C_5H_4), 4.28 (s, 5H, C_5H_5).

Ferrocenylaniline Derivatives. 2-Chloro-5-ferrocenylaniline (**b5**) was prepared according to the literature.[15] A mixture of **a5** (1.00 g, 2.93 mmol) and tin (3.94 g, 33.2 mmol) in 1:1 hydrochloric acid/ethanol (100 mL) was stirred under reflux for 1 h. The resulting orange solution was then cooled to room temperature and neutralized with aqueous sodium hydroxide. Dichloromethane was added, the solution was filtered with Celite, and the organic layer was separated. The aqueous layer was extracted with dichloromethane. The combined organic extracts were dried over sodium sulfate and filtered. Removal of the solvent followed by recrystallization from dichloromethane/hexane yielded 3-ferrocenylaniline as a yellow solid. Yield: 69% (0.63 g, 2.0 mmol). ^{1}H NMR (270 MHz, $CDCl_3$): δ 7.15 (d, $J = 8.4$ Hz, 1H, C_6H_3), 6.88−6.82 (m, 2H, C_6H_3), 4.57 (t, $J = 1.9$ Hz, 2H, C_5H_4), 4.29 (t, $J = 1.9$ Hz, 2H, C_5H_4), 4.04 (s, 5H, C_5H_5).

Similarly, 4-chloro-3-ferrocenylaniline (**b6**) and 3-ferrocenyl-4-toluidine (**b7**) were prepared in yields of 91% (1.34 g) from **a6** (1.61 g, 4.71 mmol) and 60% (0.85 g) from **a7** (1.42 g, 4.41 mmol), respectively. *Data for **b6***. ^{1}H NMR (270 MHz, $CDCl_3$): δ 7.11 (d, $J = 8.6$ Hz, 1H, C_6H_3), 6.96 (d, $J = 2.7$ Hz, 1H, C_6H_3), 6.50 (dd, $J = 8.6, 2.7$ Hz, 1H, C_6H_3), 4.72 (t, $J = 1.9$ Hz, 2H, C_5H_4), 4.31

(13) Nesmeyanov, A. N.; Perevalova, E. G.; Golovnya, R. V.; Shilovtseva, L. S. *Dokl. Akad. Nauk S. S. S. R.* **1955**, *102*, 535−538.
(14) Roberts, R. M. G.; Silver, J.; Yamin, B. *J. Organomet. Chem.* **1984**, *270*, 221−228.
(15) Campo, J. A.; Cano, M.; Heras, J. V.; Lòpez-Garabito, C.; Pinilla, E.; Torres, R.; Rojo, G.; Agulló-López, F. *J. Mater. Chem.* **1999**, *9*, 899−907.
(16) Roberts, R. M. G.; Silver, J.; Yamin, B. M.; Drew, M. G. B.; Eberhardt, U. *J. Chem. Soc., Dalton Trans.* **1988**, 1549−1556.
(17) Lanez, T.; Pauson, P. L. *J. Chem. Soc., Perkin Trans. 1* **1990**, 2437−2442.
(18) Patoux, C.; Coudret, C.; Launay, J.-P.; Joachim, C.; Gourdon, A. *Inorg. Chem.* **1997**, *36*, 5037−5049.
(19) Little, W. F.; Reilley, C. N.; Johnson, J. D.; Lynn, K. N.; Sanders, A. P. *J. Am. Chem. Soc.* **1964**, *86*, 1376−1381.
(20) Nesmeyanov, A. N. *Proc. R. Soc. London* **1955**, *246*, 495−503.
(21) Sawamura, M.; Sakaki, H.; Nakata, T.; Ito, Y. *Bull. Chem. Soc. Jpn.* **1993**, *66*, 2725−2729.
(22) Lutz, R. E.; Lytton, M. R. *J. Org. Chem.* **1937**, *2*, 68−75.
(23) Conway, B. G.; Rausch, M. D. *Organometallics* **1985**, *4*, 688−693.
(24) Horikoshi, T.; Kubo, K.; Nishihara, H. *J. Chem. Soc., Dalton Trans.* **1999**, 3355−3360.

(t, $J = 1.9$ Hz, 2H, C_5H_4), 4.12 (s, 5H, C_5H_5), 3.66 (br, 2H, NH_2). *Data for* ***b7***. ^{1}H NMR (270 MHz, $CDCl_3$): δ 7.04 (d, $J = 13.5$ Hz, 1H, C_6H_3), 6.71 (d, $J = 13.5$ Hz, 2H, C_6H_3), 4.64 (t, $J = 1.9$ Hz, 4H, C_5H_4), 4.31 (t, $J = 1.9$ Hz, 4H, C_5H_4), 4.08 (s, 10H, C_5H_5), 3.76 (br, 2H, NH_2).

2-Amino-4-ferrocenylphenol Hydrochloride (b8). A mixture of **a8** (1.00 g, 3.09 mmol) and tin powder (1.00 g, 8.42 mmol) in 1:1 hydrochloric acid/ethanol (20 mL) was stirred under reflux for 1 h. The resulting deep reddish solution was cooled, and orange solid was precipitated. The solid was filtered off and washed with a small portion of cold methanol and chloroform. Yield: 74% (0.75 g, 2.28 mmol). ^{1}H NMR (270 MHz, $CDCl_3$): δ 7.47−7.43 (m, 2H, C_6H_3), 6.94 (d, $J = 8.1$ Hz, 1H, C_6H_3), 4.63 (br, 2H, C_5H_4), 4.32 (br, 2H, C_5H_4), 4.03 (s, 5H, C_5H_5).

4-Amino-2-ferrocenylphenol Hydrochloride (b9). This compound was prepared using **a9** (0.99 g, 3.06 mmol) in a manner similar to that described for **b8**. Yield: 49% (492 mg, 1.49 mmol). ^{1}H NMR (270 MHz, CD_3OD): δ 7.47 (d, $J = 2.7$ Hz, 1H, C_6H_3), 7.03 (dd, $J = 8.6$, 2.7 Hz, 1H, C_6H_3), 6.89 (d, $J = 8.6$ Hz, 1H, C_6H_3), 4.35 (br, 2H, C_5H_4), 4.06 (s, 5H, C_5H_5).

3-Ferrocenylazobenzene (1) and its Isomer and Derivatives. A mixture of **b1** (1.40 g, 5.05 mmol) and nitrosobenzene (1.02 g, 9.53 mmol) in glacial acetic acid (30 mL) was stirred at room temperature for 24 h. The solvent was removed in vacuo, and the dark solid was purified by column chromatography with 1:1 hexane/dichloromethane as the eluent. After the first band was collected, a deep-purple solid obtained upon evaporation was recrystallized from dichloromethane/hexane. Yield: 24% (437 mg, 1.19 mmol). Anal. Calcd for $C_{22}H_{18}N_2Fe$: C, 72.15; H, 4.95; N, 7.65. Found: C, 72 44; H, 5.09; N, 7.83. ^{1}H NMR (270 MHz, CD_3CN): δ 7.94−7.87 (m, 3H), 7.63−7.42 (m, 5H), 7.30 (t, $J = 8.1$ Hz, 1H), 4.80 (t, $J = 1.9$ Hz, 2H, C_5H_4), 4.40 (t, $J = 1.9$ Hz, 2H, C_5H_4), 4.02 (s, 5H, C_5H_5).

Similarly, **4**, **5**, **6**, and **7** were prepared in 30% yield (242 mg) from **b4** (625 mg, 2.01 mmol), 19% yield (327 mg) from **b5** (1.34 g, 4.30 mmol), 20% yield (202 mg) from **b6** (850 mg, 2.65 mmol), and 21% yield (478 mg) from **b7** (191 mg, 0.41 mmol), respectively. *Data for* ***4***. Anal. Calcd for $C_{32}H_{26}N_2Fe_2$: C, 69.85; H, 4.76; N, 5.09. Found: C, 69.77; H, 4.76; N, 5.10. ^{1}H NMR (270 MHz, CD_3CN): δ 7.98−7.59 (m, 8H), 4.90 (t, $J = 1.9$ Hz, 4H, C_5H_4), 4.41 (t, $J = 1.9$ Hz, 4H, C_5H_4), 4.09 (s, 10H, C_5H_5). *Data for* ***5***. Anal. Calcd for $C_{22}H_{17}N_2ClFe$: C, 65.95; H, 4.28; N, 6.99. Found: C, 65.77; H, 4.48; N, 6.84. ^{1}H NMR (270 MHz, CD_3CN): δ 8.00−7.96 (m, 2H), 7.78 (d, $J = 2.4$ Hz, 1H), 7.69−7.53 (m, 5H), 4.76 (t, $J = 1.9$ Hz, 2H, C_5H_4), 4.38 (t, $J = 1.9$ Hz, 2H, C_5H_4), 4.05 (s, 5H, C_5H_5). *Data for* ***6***. Anal. Calcd for $C_{22}H_{17}N_2ClFe$: C, 65.95; H, 4.28; N, 6.99. Found: C, 65.97; H, 4.41; N, 6.96. ^{1}H NMR (270 MHz, CD_3CN): δ 8.32 (d, $J = 2.4$ Hz, 1H), 7.95 (m, 2H), 7.71 (dd, $J = 8.6$, 2.4 Hz, 1H), 7.63−7.53 (m, 4H), 4.86 (t, $J = 1.9$ Hz, 2H, C_5H_4), 4.42 (t, $J = 1.9$ Hz, 2H, C_5H_4), 4.18 (s, 5H, C_5H_5). *Data for* ***7***. Anal. Calcd for $C_{23}H_{20}N_2Fe$: C, 72.65; H, 5.30; N, 7.37. Found: C, 72.44; H, 5.40; N, 7.34. ^{1}H NMR (270 MHz, CD_3CN): δ 8.30 (d, $J = 1.9$ Hz, 1H, C_6H_3), 7.95−7.90 (m, 2H, C_6H_5), 7.67 (dd, $J = 8.1$, 1.9 Hz, 1H, C_6H_3), 7.62−7.50 (m, 3H, C_6H_5), 7.33 (d, $J = 8.1$ Hz, 1H, C_6H_3), 4.63 (t, $J = 1.9$ Hz, 2H, C_5H_4), 4.38 (t, $J = 1.9$ Hz, 2H, C_5H_4), 4.16 (s, 5H, C_5H_5), 2.46 (s, 3H, CH_3).

4-Ferrocenylazobenzene (2). This compound was prepared in the way described for **a5** but starting from 4-aminoazobenzene. Because of 4-aminoazobenzene's low solubility in the water/hydrochloric acid mixture, 4.20 g of 4-aminoazobenzene was dissolved in a mixture of 10 mL of acetic acid and 10 mL of sulfuric acid, whereupon it was diazotized. Yield: 17% (1.33 g, 3.63 mmol). Anal. Calcd for $C_{22}H_{18}N_2Fe$: C, 72.15; H, 4.95; N, 7.65. Found: C, 72.16; H, 5.01; N, 7.68. ^{1}H NMR (500 MHz, CD_3CN): δ 7.90 (d, $J = 8.0$ Hz, 2H), 7.85 (d, $J = 8.5$ Hz, 2H), 7.70 (d, $J = 8.5$ Hz, 2H), 7.59−7.50 (m, 3H), 4.82 (t, $J = 2.0$ Hz, 2H, C_5H_4), 4.43 (t, $J = 2.0$ Hz, 2H, C_5H_4), 4.06 (s, 5H, C_5H_5).

5-Ferrocenyl-2-hydroxyazobenzene (8). A mixture of **b8** (492 mg, 1.49 mmol) and **5** (160 mg, 1.50 mmol) in a small portion of triethylamine and glacial acetic acid was stirred at room temperature for 24 h. The solvent was removed in vacuo, and the dark solid was purified by column chromatography with an increasing proportion of chloroform in hexane as an eluent. The second band, which was eluted with hexane/chloroform (1:2), was collected and recrystallized from dichloromethane/hexane. Yield: 23% (131 mg, 0.343 mmol). Anal. Calcd for $C_{22}H_{18}N_2OFe$: C, 69.13; H, 4.75; N, 7.33. Found: C, 69.04; H, 4.83; N, 7.33. ^{1}H NMR (270 MHz, $CDCl_3$): δ 12.85 (s, 1H, OH), 8.04 (d, $J = 2.2$ Hz, 1H), 7.91 (dd, $J = 8.1$, 1.6 Hz, 2H), 7.59−7.48 (m, 4H), 6.99 (d, $J = 8.6$ Hz, 1H), 4.67 (t, $J = 1.9$ Hz, 2H, C_5H_4), 4.33 (t, $J = 1.9$ Hz, 2H, C_5H_4), 4.08 (s, 5H, C_5H_5).

3-Ferrocenyl-4-hydroxyazobenzene (9). 9 was prepared from **b9** (488 mg, 1.48 mmol) in a manner similar to that of **8**. Yield: 30% (170 mg, 0.44 mmol). Anal. Calcd for $C_{22}H_{18}N_2OFe$: C, 69.13; H, 4.75; N, 7.33. Found: C, 68.46; H, 4.86; N, 7.12. ^{1}H NMR (270 MHz, CD_3CN): δ 8.07 (d, $J = 2.4$ Hz, 1H), 7.89−7.85 (m, 2H), 7.71 (dd, $J = 8.4$, 2.4 Hz, 1H), 7.59−7.46 (m, 3H), 7.02 (d, $J = 8.4$ Hz, 1H), 4.83 (t, $J = 1.9$ Hz, 2H, C_5H_4), 4.38 (t, $J = 1.9$ Hz, 2H, C_5H_4), 4.07 (s, 5H, C_5H_5).

4-(3-Ferrocenyl-phenylazo)phenyl *p*-Toluenesulfonate (10). 4-Nitrosophenol *p*-toluenesulfonate was prepared from 4-nitrophenol *p*-toluenesulfonate[21] (3 g, 10.2 mmol), and a mixture containing unreacted 4-nitrophenol *p*-toluenesulfonate was used in the next step. **10** was obtained from mixing 4-nitrosophenol *p*-toluenesulfonate and 3-ferrocenylaniline in acetic acid and chloroform. The crude product was purified using silica column chromatography in hexane/chloroform (1:1) and then was recrystallized from dichloromethane/hexane. Anal. Calcd for $C_{29}H_{25}FeN_2O_3S$: C, 64.93; H, 4.51; N, 5.22. Found: C, 64.82; H, 4.68; N, 5.18. ^{1}H NMR ($CDCl_3$): δ 2.441 (s, 3H), 4.05 (s, 5H), 4.35 (s, 2H), 4.72 (s, 2H), 7.13 (d, $J = 6.93$, 2H), 7.31 (d, $J = 8.25$, 2H), 7.40 (t, $J = 7.918$, 1H), 7.58 (d, $J = 8.25$, 2H), 7.68 (d, $J = 7.92$, 1H), 7.86 (d, $J = 8.91$, 2H), 7.97 (s, 1H).

4-(3-Ferrocenylphenylazo)-phenol (11).[25] Under a nitrogen atmosphere, a mixture of **10** (1 g, 1.9 mol) and potassium hydroxide (2.2 g, 22.2 mol) in ethanol (36 mL) and water (36 mL) was stirred under reflux for 1 h. The resulting orange solution was then cooled to room temperature and neutralized with hydrochloric acid. Diethyl ether was added and then filtered with Celite, and the organic layer was separated. The aqueous layer was extracted with diethyl ether. The combined organic extracts were dried over sodium sulfate and filtered. Removal of the solvents followed by recrystallization from dichloromethane/hexane yielded an orange solid. Yield: 79% (0.56 g, 0.44 mmol). Anal. Calcd for $C_{22}H_{18}FeN_2O$: C, 66.02; H, 5.04; N, 7.00. Found: C, 66.11; H, 4.95; N, 6.90. ^{1}H NMR ($CDCl_3$): δ 4.05 (s, 3H), 4.34 (s, 5H), 4.72 (s, 2H), 5.28 (s, 2H), 6.95 (d, $J = 8.58$, 2H), 7.39 (t, $J = 7.59$, 1H), 7.54 (d, $J = 7.59$, 1H), 7.67 (d, $J = 8.58$, 1H), 7.89 (d, $J = 8.91$, 2H), 7.96 (s, 1H).

[4-(2-Bromo-octyloxy)-phenyl]-(3-ferrocenyl-phenyl)diazene (12).[26] Under a nitrogen atmosphere, **11** (500 mg, 1.3 mol), potassium carboxide (0.5 g, 5.0 mol), and 1,8-dibromooctane

(25) Wolfrom, M. L.; Koos, E. W.; Bhat, H. B. *J. Org. Chem.* **1967**, *32*, 1058−1060.
(26) Boden, N.; Bushby, R. J.; Martim, P. S.; Evans, R. W.; Smith, D. A. *Langmuir* **1999**, *15*, 3790−3797.

(25 mL, 62.7 mmol) in dried ethanol (100 mL) were stirred and kept at 60 °C for 24 h. The resulting orange solution was then cooled to room temperature. Dichloromethane was added and then filtered with Celite, and the organic layer was separated. The aqueous layer was extracted with dichloromethane. The combined organic extracts were dried over sodium sulfate and filtered. The dark solid was purified by column chromatography with an increasing proportion of dichloromethane in hexane as an eluent. Removal of the solvent followed by recrystallization from dichloromethane/hexane yielded an orange solid. Yield: 81% (0.60 g, 0.44 mmol). Anal. Calcd for $C_{30}H_{33}BrFeN_2O$: C, 62.85; H, 5.80; N, 4.89. Found: C, 63.06; H, 5.81; N, 4.70. ^{1}H NMR ($CDCl_3$): δ 3.40 (s, 2H), 4.03 (s, 5H), 4.35 (s, 2H), 4.73 (s, 2H), 5.28 (s, 1H), 6.99 (d, J = 8.91, 1H), 7.39 (t, J = 7.59, 1H), 7.53 (d, J = 6.93, 1H), 7.68 (d, J = 7.56, 1H), 7.92 (d, J = 8.90, 1H), 7.953 (s, 1H). MALDI−TOF MS (m/z): 571.77 = M^+ (M_w = 572.11).

8-[4-(3-Ferrocenylazo)phenoxy]octyl Disulfide (13).[27] Under a nitrogen atmosphere, **12** (100 mg, 0.17 mmol) and thiourea (141.2 mg, 1.8 mmol) were stirred into dried ethanol (10 mL) and kept at 80 °C for 72 h. Then, tetraethylenepentamine (0.35 mL, 1.9 mmol) was added and stirred for 8 h. The resulting orange solution was then cooled to room temperature. Dichloromethane was added and then filtered with Celite, and the organic layer was separated. The aqueous layer was extracted with dichloromethane. The combined organic extracts were dried over sodium sulfate and filtered. The orange solid was purified by column chromatography with an increasing proportion of dichloromethane in hexane as an eluent. Removal of the solvent followed by recrystallization from hexane yielded an orange solid. Yield: 18% (32.2 mg, 0.44 mmol). Anal. Calcd for $C_{60}H_{66}FeN_2OS_2 \cdot H_2O$: C, 67.41; H, 6.41; N, 5.24. Found: C, 67.66; H, 6.46; N, 4.78. ^{1}H NMR ($CDCl_3$): δ 2.62 (t, J = 7.4, 2H), 3.97 (t, J = 6.4, 2H), 4.33 (s, 2H), 4.72 (s, 2H), 6.74 (d, J = 9.2, 1H), 7.33 (t, J = 7.8, 1H), 7.47 (d, J = 7.6, 1H), 7.58 (d, J = 8.00, 1H), 7.84 (d, J = 8.80, 2H), 7.87 (s, 1H).

{**8-[4-(3-Ferrocenyl-phenylazo)-phenoxy]-octyl**}**-phosphonic Acid Diethyl Ester (14). 12** (200 mg, 0.35 mmol) was refluxed at 170 °C in triethyl phosphite (20 mL) for 3 days. After cooling to room temperature, the triethyl phosphite was removed under a vacuum. The orange solid was purified by column chromatography with dichloromethane. Removal of the solvent followed by recrystallization from dichloromethane/hexane (1:1) yielded a yellow solid. Yield: 46% (102 mg, 0.16 mmol). Anal. Calcd for $C_{34}H_{43}FeN_2O_4P$: C, 64.76; H, 6.78; N, 4.44. Found: C, 64.61; H, 6.82; N, 4.36. ^{1}H NMR ($CDCl_3$): δ 2.62 (t, J = 7.4, 2H), 3.97 (t, J = 6.4, 2H), 4.33 (s, 2H), 4.72 (s, 2H), 6.74 (d, J = 9.2, 1H), 7.33 (t, J = 7.8, 1H), 7.47 (d, J = 7.6, 1H), 7.58 (d, J = 8.00, 1H), 7.84 (d, J = 8.80, 2H), 7.87 (s, 1H).

Determination of Photoisomerization Quantum Yields. A 10 mm light path length quartz cell was used to measure photoisomerization. The sample solution was degassed by N_2 bubbling before photoirradiation. According to the literature,[28] the quantum yield of trans-to-cis photoisomerization ($\Phi_{t\rightarrow c}$) and that of cis-to-trans ($\Phi_{c\rightarrow t}$) are described in the following equations:

$$p_{\lambda_i} = \epsilon_t(\lambda_i)\Phi_{t\rightarrow c} + \epsilon_c(\lambda_i)\Phi_{c\rightarrow t}$$

where $A_{\lambda_i}(t,\lambda_o)$ designates the absorbance of the solution irradiated

$$A_{\lambda_i}(t_n,\lambda_o) = A_{\lambda_i}(\infty,\lambda_o) - [A_{\lambda_i}(\infty,\lambda_o) - A_{\lambda_i}(0,\lambda_o)]\, e^{-p_{\lambda i} I_{\lambda i} \Theta(t_n)}$$

$$\Theta(t_n) = \int_0^{t_n} dt \frac{1 - 10^{-A_{\lambda i}(t,\lambda_i)}}{A_{\lambda_i}(t,\lambda_i)}$$

with light of wavelength λ_i measured at the observation wavelength λ_o as a function of the irradiation time t. Furthermore, $\epsilon_t(\lambda_i)$ and $\epsilon_c(\lambda_i)$ denote the molar absorption coefficients of the trans and cis forms, respectively, measured at wavelength λ_i, and I_{λ_i} is the intensity of the incident light. From these equations, the parameter p_{λ_i} can be obtained. And we can obtain the equation $c_t/c_c = \epsilon_c\Phi_{c\rightarrow t}/\epsilon_t\Phi_{t\rightarrow c}$, where c_t and c_c denote the trans and cis molar ratios in the PSS, respectively. If the cis molar ratio in the PSS is known, ϵ_c can be calculated from the absorption spectrum of the trans form and from that in the PSS, so that only the parameter p_{λ_i} is needed to obtain $\Phi_{t\rightarrow c}$. The intensity of the light was determined by using $K_3[Fe(C_2O_4)_3]$ as a chemical actinometer.[29]

Electrochemical Measurements. A glassy carbon rod (outside diameter 5 mm, Tokai Carbon GC-20) was embedded in Pyrex glass, and the cross-section was used as a working electrode. Cyclic voltammetry was carried out in a standard one-compartment cell under an argon atmosphere equipped with a platinum-wire counter electrode and an Ag/Ag^+ reference electrode [10 mM $AgClO_4$ in 0.1 M n-Bu_4ClO_4−acetonitrile solution, $E^{0\prime}$(ferrocenium/ferrocene) = 0.210 V vs Ag/Ag^+] with a BAS CV-50W or an ALS 750A voltammetric analyzer. Controlled-potential electrolysis was carried out with an electrochemical spectroscopic quartz cell equipped with a Pt mesh working electrode, a Pt wire counter electrode, and the Ag/Ag^+ reference electrode with a Toho Technical Research PS-14 Potentiostat.

Crystal Structure Determination. All measurements were made on a Rigaku AFC8 diffractometer coupled with a CCD area detector with graphite-monochromated Mo Kα radiation (0.7107 Å). The structure was solved by direct methods and expanded using Fourier techniques. Hydrogen atoms were not included in the calculations. All calculations were performed using the Crystal Structure crystallographic software package (Rigaku Corp. and Molecular Structure Corp.). **1** was formed as a red-plate crystal by evaporation of dichloromethane. This crystal, with approximate dimensions of 0.20 × 0.20 × 0.20 mm, was mounted on a glass loop. The crystals of **11** were grown as red plates by vapor-diffusion evaporation of an ethanol/hexane solution (1:1). These crystals, with approximate dimensions of 0.40 × 0.30 × 0.10 mm each, were mounted on a glass loop. **5** was crystallized as a dark red block by vapor-diffusion evaporation of dichloromethane and hexane (1:1). This crystal, with approximate dimensions of 0.40 × 0.20 × 0.10 mm, was mounted on a glass loop.

DFT Calculations. The three-parametrized Becke−Lee−Yang−Parr (B3LYP) hybrid exchange-correlation functional was employed. For comparisons with the UV−visible absorption spectra observed in acetonitrile, the solvent effect was taken into account by means of the polarized continuum model. The core electrons of Fe and the first-row elements were replaced with effective core potentials (ECPs), and their valence orbitals were described with the double-ζ basis set prepared for the ECPs. For hydrogen, the 4-31G basis set was used. The geometries of these compounds were optimized with the DFT(B3LYP) method without the solvent effect. The present calculations were implemented with the Gaussian98 (rev. A7) program.

(27) Wang, R.; Iyoda, T.; Tryk, D. A.; Hashimoto, K.; Fujishima, A. *Langmuir* **1997**, *13*, 4644−4651.
(28) Wettermark, G.; Langmuir, M. E.; Anderson, D. G. *J. Am. Chem. Soc.* **1965**, *87*, 476−481.
(29) Gade, R.; Porada, T. *J. Photochem. Photobiol., A* **1997**, *107*, 27−34.

Acknowledgment. This work was supported by Grants-in-Aid for Scientific Research [Grants 15033215 (area 417) and 14204066] and by a grant from The 21st Century COE Program for Frontiers in Fundamental Chemistry from MEXT, Japan.

Supporting Information Available: A scheme for the synthesis of compounds, ORTEP diagrams of **5** and **11** (Figure S1), ^{1}H NMR spectra (Figure S2), cyclic voltammogram (Figure S3), UV−vis spectral change upon oxidation (Figure S4) and upon protonation of **1** (Figures S5 and S6), ^{1}H NMR spectra (Figure S7) and cyclic voltammogram (Figure S8), UV−vis spectral change upon oxidation (Figure S9) and upon protonation of **2** (Figures S10 and S11), UV−vis spectral change upon photoirradiation (Figure S12), and ^{1}H NMR spectra of **3** (Figure S13). Crystallographic and geometric data in CIF format. This material is available free of charge via the Internet at http://pubs.acs.org.

IC051184R